1-1-1981

The effects of load ration on environmentally assisted fatigue crack growth.

True-Hwa Shih

THE EFFECTS OF LOAD RATION ON ENVIRONMENTALLY ASSISTED FATIGUE CRACK GROWTH

by

True-Hwa Shih

A Thesis

Presented to the Graduate Committee

of Lehigh University

in Candidacy for the Degree of

Master of Science

in

Mechanical Engineering

Lehigh University

1981

This thesis is accepted and approved in partial fulfillment of the requirements for the degree of Master of Science.

August 12, 1981
(date)

Professor in Charge

Chairman of Department

ACKNOWLEDGMENTS

The author wishes to express his gratitude to Professor R. P. Wei for his instruction, his guidance, especially for his support and patience. The author also expresses his appreciation to Mr. C. D. Miller and Mr. R. L. Brazill for their technical assistance in the experimental work; to Mrs. Shirley Simmons for the typing of the equations; to his wife for her encouragement and the typing of the manuscript. Partial support of this research by the Air Force Office of Scientific Research under contract No. F49620-81-K-0004 is acknowledged.

TABLE OF CONTENTS

LIST OF FIGURES

LIST OF TABLES

ABSTRACT

A modification to the model of Weir et al. for surface reaction and transport controlled fatigue crack growth has been developed to explicitly account for the effect of load ratio on environmentally assisted fatigue crack growth. Load ratio was found to affect principally gas transport to the crack tip, and therefore affected only transport controlled crack growth response. Experimental verification of the modified model was made by studying the room temperature fatigue crack growth responses at different load ratios for a 2219-T851 aluminum alloy exposed to water vapor.

The results show that the effects of load ratio can be attributed to two different sources - one relating to its effect on local deformation at the crack tip and is reflected through the mechanical component, $(da/dN)_r$, and the other on its role in modifying environmental effect and is manifested through the corrosion fatigue component, $(da/dN)_{cf}$. Furthermore, the results show that the saturation value of corrosion fatigue component, $(da/dN)_{cf,s}$, is essentially independent of R, and that the exposure needed to produce "saturation response", $(p_o/2f)_s$, as a function of load ratio can be predicted from the modified model. The modified model, therefore, allows one to predict the corrosion fatigue crack growth response for any load ratio on the basis of measurements made at a single load ratio, provided that the values of $(da/dN)_r$ are known .

I. INTRODUCTION

Fatigue crack growth is an important engineering problem of long standing, especially under the conjoint actions of mechanical fatigue and chemical attack. It is one of the principal factors that govern the reliability and serviceable lives of engineering structures. Fatigue crack growth has been shown to be a function of both stress intensity factor range, ΔK, and maximum stress intensity factor, K_{max}, or of ΔK and load ratio R, where $\Delta K = K_{max} - K_{min}$ and $R = K_{min}/K_{max}$[1] in one load cycle [1-3]. A number of empirical relations have been developed to account for the influence of load ratio [1,3-6]. Being based on continuum mechanics, these empirical relations can deal, at best, with the influence of local deformation. It is now recognized that the influence of load ratio may be attributed to two different sources -- one relating to its effect on local deformation at the crack tip, and the other on its role in modifying environmental effects. At a given ΔK level, the presence of a mean load contributes to additional local deformation, so that the crack growth rate can be expected to increases with increasing load

---

[1]The load ratio R is defined as the ratio between minimum and maximum loads in a given cycle. The definition used here, in a strict sense, only applies to those cases where $K_{min} > 0$.

ratio, R. This increase in rate with R has been verified experimentally [1,3-6]. By the same token, the effective crack opening at the same ΔK level, (or the same K_{max} level), will be larger for the higher R values. This change in effective crack opening will affect the transport of gases to the crack tip and thereby alter crack growth response.

The effect of R on environment assisted crack growth has not been considered and will be examined in this thesis. A model for surface reaction and transport controlled fatigue crack growth [7], developed and experimentally verified recently, will be used. This model is able to account for the influence of gas pressure and cyclic load frequency on the rate of fatigue crack growth. However, it did not explicitly incorporate the influences of load ratio. To broaden the applicability of this model, modifications to incorporate the influences of load ratio will be developed and will be verified experimentally.

The development of the model for surface reaction and transport controlled fatigue crack growth is first briefly reviewed. Necessary modifications are made based on the consideration of different load ratios and actual wave form of the applied load. To verify the effects of load ratio on environment assisted crack growth, fatigue crack growth experiments have been carried out under sinusoidal loading with different load ratios on an Al-Cu

alloy (2219-T851 aluminum alloy) in water vapor and dehumidified argon at room temperature. Experimental results are then reported, and are discussed in terms of the modified model.

II. MODELING OF FATIGUE CRACK GROWTH

Modeling of environment assisted fatigue crack growth was based on the proposition that the rate of crack growth in an aggressive environment, $(da/dN)_e$, is composed of the sum of two components, when the contribution from sustained-load crack growth is negligible [2,7,8,9].

$$(da/dN)_e = (da/dN)_r + (da/dN)_{cf} \quad (1)$$

In equation(1), $(da/dN)_r$ is the rate of crack growth in an inert environment and represents the contribution of "pure" (mechanical) fatigue; and $(da/dN)_{cf}$ is the cycle-dependent environmental contribution, or the corrosion fatigue component, which requires the conjoint action of fatigue and environmental attack.

An one-dimensional model was developed by Weir et al. [7], and modified by Wei and Simmons [8], to account for the influences of environmental variables on $(da/dN)_{cf}$. Development of this model is briefly summarized to provide background for the proposed modification for R effect [7-10]. The following assumptions were made [7,8]

1. The environmental contribution to the rate of fatigue crack growth, $(da/dN)_{cf}$, is assumed to be proportional to the amount of embrittling

species (hydrogen) produced by the surface reactions during each loading cycle , and is thus proportional to the product of the "effective" crack area and the extent of surface reaction.

2. The reactive surface (new crack surface) is assumed to form instantaneously at the maximum load, and the geometry of the crack is assumed to remain fixed until unloading. The time available for reaction is thus taken to be one-half of the fatigue cycle.
3. The rates of diffusion and embrittlement are assumed to be much faster than those of gas transport and of the surface reactions, and therefore do not need to be considered. Gas transport, at low pressure, is assumed to be described by molecular or Knudsen flow [12]

The governing differential equations for flow and surface reactions are as follows [7,8]:

$$\frac{dp}{dt} = - \frac{SN_o kT}{V} \frac{d\theta}{dt} + \frac{F}{V}(p_o - p) \qquad (2)$$

$$\frac{d\theta}{dt} = k_c p f(\theta) = k_c p (1 - \theta) \qquad (3)$$

The terms in the equations are as follows:

$F = 8.72 \times 10^2 \beta(\sigma_{ys}/E)^2 (T/M)^{1/2} B\ell$ (in m^3/s)
= Knudsen flow parameter that depends on dimension and shape of the capillary, molecular weight (M) of the gas and temperature (T). The specific form of this expression reflects an attempt to account for constriction in flow by the real crack, where σ_{ys} is the yield strength, E is the Young's modulus and B is the specimen thickness, ℓ is a selected distance (of the order 10^{-6}m) from the crack tip used in defining a crack opening, and β is an empirical quantity to be determined from the crack growth data [8,11]

k_c = reaction rate constant, $(Pa\text{-}s)^{-1}$

N_o = density of surface sites; molecules (atoms)-m^{-2}

p = pressure of gas at the crack tip; Pa.

p_o = pressure of gas in the surrounding environment; Pa.

k = Boltzmann constant = 1.38×10^{-23} Pa-m^3-molecules^{-1}-K^{-1}.

$S = \alpha(2B\Delta a^*)$ = area of "effective" crack surface per cycle, where Δa^*= "effective" crack increment , B = specimen thickness, and α = empirical constant for surface roughness and crack geometry [8].

T = absolute temperature.

V = control volume at the crack tip, i.e., volume associated with the distance ℓ.

θ = fractional surface coverage or extent of reaction of surface per unit area.

From equation (2), it can be seen that the rate of change of pressure at the crack tip depends on the decrease in pressure produced by reaction of the environment with the active ("effective") crack surface and on the increase in pressure from the influx of gas

from the external environment. The form $f(\theta) = 1 - \theta$ in equation (3) incorporates the assumption that the surface reaction is fist-order in relation to available surface sites [3,4].

Solutions for equations (2) and (3), with $f(\theta) = 1 - \theta$, were obtained for two limiting cases, for $0 < \theta < 1$, and were used in conjunction with assumption 1 to estimate the influences of key environmental and loading variables on the cycle-dependent component of fatigue crack growth rate, i.e., on $(da/dN)_{cf}$ [7-10].

Case I: Transport controlled.

$$\theta \approx \frac{F}{SN_o kT} p_o t \qquad \text{for} \quad \frac{SN_o kTk_c}{F} >> 1 \tag{4}$$

Case II: Surface reaction controlled.

$$\theta \approx 1 - \exp(- k_c p_o t) \qquad \text{for} \quad \frac{SN_o kTk_c}{F} << 1 \tag{5}$$

In the transport controlled case, because of the rapid reactions of the environment with the freshly created crack surfaces (high k_c) and the limited rate of supply of the environment to the crack tip, significant attenuation of gas pressure takes place at the crack tip (see Figs. 1 and 2). The extent of surface reaction (θ), see equation (4), during one cycle is controlled by the rate of transport of the aggressive environment to the crack tip, and thereby varies linearly with time. For

the surface reaction controlled case, the reaction rates are sufficiently slow so that the gas pressure at the crack tip is essentially equal to the external pressure. The extent of reaction, for $f(\theta) = 1 - \theta$, becomes an exponential function of time, equation (5).

To explicitly incorporate the effect of load ratio, it is necessary to reconsider the flow parameter in the model [8,9]. As in the original model [7], for estimating the flow parameter F, it is most convenient to treat the crack as an equivalent rectangular channel , with an effective opening δ , an effective length L, and a width equal to the specimen thickness B. Based on Knudsen flow [12], F for the rectangular channel is given by equation (6).

$$F \approx \frac{4}{3} V_a \left[\frac{\delta^2 B}{2L}\right] \tag{6}$$

where $V_a = 1.45 \times 10^2 (T/M)^{1/2}$ (m/s) is the r.m.s. (root mean square) velocity of the gas molecules .

To provide a consistent basis for comparison and to properly reflect the influence of cyclic loading, the effective opening is given in terms of an effective elastic crack opening at a distance ℓ from the crack tip [12], modified by a multiplicative constant . To account for the fact that the crack opening varies during cyclic loading and the average effect of δ^2 on F (see equation (6)), the r.m.s. value of elastic crack opening for

sinusoidal loading is used here, in place of that based on K_{max} in the original model [7,8] (see appendix).

$$\delta_{rms} = \beta_1^* \frac{3K_{max}}{E} \sqrt{\ell} \cdot \frac{1}{2} \left[(1 + R)^2 + \frac{1}{2} (1 - R)^2 \right]^{1/2} \qquad (7)$$

The constant β_1^* is assumed to provide adequate correction for crack geometry, including the effect of local plastic deformation.

It is necessary also to redefine the effective flow length. Constriction in flow is believed to result from local plastic deformation, associated with the process of crack growth, in the wake of the crack. The local deformation is expected to be confined within the crack tip plastic zone. As such, it is reasonable to assume that the length of flow constriction is related to the cyclic plastic zone size. Therefore the effective flow length is redefined in terms of the cyclic plastic zone. (i.e., one based on ΔK), in place of that based on K_{max} in the original model [7].

$$L = \beta_2^* \left(\frac{\Delta K}{\sigma_{ys}} \right)^2 \qquad (8)$$

The parameter β_2^* is again assumed to be a constant, which includes an appropriate coefficient for the cyclic plastic zone, and σ_{ys} is the yield strength of the alloy.

On the basis of these assumption, the flow parameter may now be given as follows:

$$F = 8.72 \times 10^2 \, \beta^* f(R) \, \frac{\sigma_{ys}^2}{E^2} \, B\ell \, \left(\frac{T}{M}\right)^{1/2} \qquad (\text{in } m^3/s)$$

$$\text{where } \beta^* = \beta_1^{*2}/\beta_2^* \,, \quad \text{and} \tag{9}$$

$$f(R) = \frac{1}{4}\left[\left(\frac{1 + R}{1 - R}\right)^2 + \frac{1}{2}\right]$$

The quantity 8.72×10^2 is a dimensioned constant, with the units of $(m^2/s)(gm/K)^{-1/2}$. The expression for F differs from that given by Weir et al. [7], and Wei and Simmons [8], in that a function f(R) is introduced here to explicitly account for the influence of load ratio. As a result, the parameters β_1^*, β_2^* and β^* assume values that are different from β_1, β_2 and β defined previously [8,9], although the physical significance of these parameters remains unchanged. In the original model, the influence of load ratio was implicitly incorporated in these parameters, whereas, in this modification the influence of load ratio is explicitly treated. Specifically, $\beta^* f(R)$ is equal to β.

Based on assumption 1, $(da/dN)_{cf} \propto \theta \Delta a^*$, and by taking the "effective" crack increment (Δa^*) along with ℓ in the expression of F to be equal to the growth increment per cycle at saturation (i.e., for $\theta = 1$, $\Delta a^* = \ell = (da/dN)_{e,s}(1)$) and t equal to 1/2f [1,3], the

following expressions can be obtained from equations (4) and (5):

Case I: Transport controlled.

$$(p_o/2f)_s \simeq \left[436 \frac{\beta^*}{\alpha} f(R) \frac{\sigma_{ys}^2}{N_o kTE^2} \left(\frac{T}{M}\right)^{1/2} \right]^{-1} \tag{10}$$

$$\frac{(da/dN)_{cf}}{(da/dN)_{e,s}} \propto 436 \frac{\beta^*}{\alpha} f(R) \frac{\sigma_{ys}^2}{N_o kTE^2} \left(\frac{T}{M}\right)^{1/2} \frac{p_o}{2f} \tag{11}$$

$$\frac{(da/dN)_{cf}}{(da/dN)_{cf,s}} = \frac{(p_o/2f)}{(p_o/2f)_s} \tag{12}$$

Case II: Surface reaction controlled.

$$\frac{(da/dN)_{cf}}{(da/dN)_{e,s}} \propto 1 - \exp(-k_c p_o/2f) \tag{13}$$

$$\frac{(da/dN)_{cf}}{(da/dN)_{cf,s}} = 1 - \exp(-k_c p_o/2f) \tag{14}$$

Subscript s is used to denote the corresponding values at saturation and "β^*/α" is an empirical parameter [8] to be determined from the fatigue crack growth experiments. The engineering significance and implications of the modified model may be discussed in relation to equations (10) to (14). The modified model provides a formalism for "predicting" environmentally assisted crack growth response in relation to load ratio, gas pressure and

cyclic load frequency. Specifically, for transport controlled case, the model shows:

- $(p_o/2f)_s$ is an explicit function of R, see equation (10), and depends also on the properties of the alloy, molecular weight of the aggressive gas and temperature.
- Below saturation $(da/dN)_{cf}$ is an explicit function of $(p_o/2f)$ and $(p_o/2f)_s$, see equation (12),and thus also depends on R.

The actual value of $(da/dN)_{cf}$ is proportional to the extent of surface reaction, i.e., on θ , see assumption 1. Since the extent of surface reaction (coverage) is limited, $(da/dN)_{cf}$ will arrive a saturation value of $(da/dN)_{cf,s}$ above a critical value of $p_o/2f$, i.e., above $(p_o/2f)_s$, for which the coverage is completed ($\theta = 1$) during each loading cycle. Thus $(da/dN)_{cf,s}$ should be independent of R at a given ΔK level. Because load ratio affects only gas transport, environmentally assisted crack growth response is not expected to depend on R for the case of surface reaction controlled growth, see equations (13) and (14). Therefore, only the transport controlled case will be examined experimentally to verify the model.

III. MATERIAL AND EXPERIMENTAL WORK

A. Material and Specimen

A 16.5 mm thick plate[2] of 2219-T851 aluminum alloy is used in this study. Nominal tensile properties of this plates are as follows: yield strength = 358 MPa and tensile strength = 455 MPa. The plane strain fracture toughness is about 36 to 41 MPa-$m^{1/2}$.

Wedge-opening-load (WOL) specimens, Fig. (2), with half-height to width ratio (H/W) of 0.486, were selected for use. The specimens were oriented in the longitudinal (LT) orientation. An initial (or crack starter) notch, 19.6 mm in length, was introduced into each specimen by electro-discharge machining (EDM). Each specimen was precracked in constant amplitude fatigue at the desired load level for the actual experiment while exposed to the test environment. The precracking procedure provided a fatigue crack of about 3.3 mm in length from the starter notch, corresponding to a crack length of about 23 mm at the start of each experiment. This precracking procedure ensured that the subsequent fatigue crack growth would be through material that had not been altered by the notch preparation procedure, and would be unaffected by the starter notch geometry.

---

[2]Plate furnished by Air Force Flight Dynamics Laboratory, WPAFB, CH.

B. Stress Intensity Factor Calibration

Stress intensity factor K for the WOL specimen was computed from equation (15) [14,15] :

$$K = \frac{P}{BW}\sqrt{a}\,[30.96 - 195.8\,(a/W) + 730.6\,(a/W)^2 - 1186.3\,(a/W)^3 + 754.6\,(a/W)^4] \qquad (15)$$

where P = applied load

B = specimen thickness

W = specimen width

a = crack length

Both specimen width and crack length were measured from the line of loading (see Fig. 3).

C. Test Environment

The crack growth experiments were carried out in dehumidified argon and in water vapor inside a commercial ultrahigh vacuum chamber, Fig. 4, at room temperature. The vacuum chamber had been modified to provide mechanical force feedthroughs and was pumped to an ultrahigh vacuum of less than 10^{-6} Pa (after bakeout) before backfilling with the selected test environment. For tests in argon, approximately 2.7 kPa (20 torr) of ultrahigh purity argon was admitted into the chamber through a cryogenic trap to remove impurities, such as water vapor. Water vapor was obtained from a high-purity water source attached as a sidearm to the vacuum chamber. Impurity level of the water vapor was estimated to be

less than 100 ppm. Pressure was monitored by a capacitance manometer and purity was verified with the aid of a quadrupole residual gas analyzer (RGA). For the test in dehumidified argon at a load ratio of 0.5, the environment was maintained around the crack by flowing argon (from a suitable purification system) at approximately 133 kPa through chambers clamped to the faces of the specimen [17].

D. Crack Monitoring System

An ac (alternating current) electrical potential system, Fig. 4, was used for monitoring crack growth [18-20]. Calibration results, (see Fig. 5), given in terms of crack length (a) versus potential difference $(V - V_r)$, can be represented by equation (16), see [19].

$$a = 19.6 + 4.03\ (V - V_r) \qquad \text{(a in mm)} \qquad (16)$$

$V = V(a)$ = potential corresponding to crack length a, and V_r = reference potential corresponding to the initial notch. Both V and V_r are given in microvolts. Accuracy of crack length measurement with the ac system was estimated to be better than 1 pct, for crack lengths from 20 to 48 mm (0.8 to 1.85 in.). The resolution was better than 0.05 mm (0.002 in.) based on 12.5 nV resolution in electrical potential.

E. Experimental Procedures

The fatigue tests were carried out under constant-load-amplitude, sinusoidal loading in a closed-loop electrohydraulic testing machine, Fig. 7, operated in load control. A programmed digital controller is interfaced with the testing machine to provide automated control and data acquisition. Load control was estimated to be better than 1 pct. Load ratios of 0.2 and 0.5 were used. Taken together with data obtained previously at R = 0.05 [9], three different load ratios are then available for verifying the proposed model for environmentally assisted crack growth. For the tests in argon, frequencies of 5 and 20 Hz were used. Tests in water vapor were carried out at 5 Hz. The tests covered stress intensity factor range (ΔK) values from about 10 MPa-$m^{1/2}$ to about 26 MPa-$m^{1/2}$.

IV. RESULTS AND DISCUSSIONS

Room temperature fatigue crack growth data obtained from tests in water vapor at pressure from 0.4 to 133 Pa (3.0×10^{-3} to 1 torr), for load ratios of 0.05 (see [9]) and 0.2 and 0.5, are shown as a function of stress intensity factor range (ΔK) in Figs. 8-10, along with data obtained from tests in dehumidified argon. These data are also shown in Figs. 11-13 as a function of water vapor pressure and $p_o/2f$ at three ΔK levels. Assuming that 1 ppm of water vapor remains as impurity in dehumidified argon, tests in dehumidified argon at 2.7 kPa would be equivalent to those in vacuum at about 2.7×10^{-3} Pa (2×10^{-5} torr), and that in argon at 133 kPa, to vacuum at 1.3×10^{-1} Pa. The dehumidified argon data are used in calculating $(da/dN)_{cf}$ (see equation (1)).

For the tests with load ratio of 0.2, the crack growth rates at 2.66 and 13.3 Pa correspond to those for maximum environmental effect or "saturation", i.e., $(da/dN)_{e,s}$. For R = 0.5, the saturation values are taken to be those corresponding to 1.0, 1.4 and 133 Pa. The average of the differences between $(da/dN)_r$ and these rates for each load ratio is taken as $(da/dN)_{cf,s}$ for that load ratio. The normalized corrosion fatigue component, $(da/dN)_{cf}/(da/dN)_{cf,s}$, are then calculated and plotted as a function of water vapor pressure for

different load ratios in Figs. 14-16. The error bands represent 95 pct confidence intervals computed from the residual standard deviations in each set of data [17,21].

The values of $(p_o/2f)_s$ for the onset of saturation response were estimated and are 0.64 Pa-s, 0.26 Pa-s, 0.10 Pa-s for load ratios of 0.05, 0.2 and 0.5 respectively (Figs. 11 to 13). These values are shown as a function of $[f(R)]^{-1}$ in Fig. 17. Least-squares regression analysis of these data showed that $(p_o/2f)_s$ is linearly proportional to $[f(R)]^{-1}$; the dependence is in agreement with the model prediction (i.e., with equation (10)). This correlation indicates that the empirical parameter β^*/α is constant and is approximately equal to 3.8. The value of $\beta^*/\alpha\, f(R)$ at R = 0.05 is 1.6 which is identical with the value of β/α given by Weir et al. [7].

From the regression analysis, values of $(p_o/2f)_s$ are found to be 0.58 Pa-s, 0.36 Pa-s and 0.11 Pa-s for load ratios of 0.05, 0.2 and 0.5, respectively. Based on these values and the modified model, curves for crack growth response are obtained from equation (13) and (14), and from the experimentally measured values of $(da/dN)_r$ and $(da/dN)_{cf,s}$. They are shown as solid lines in Figs. 11-16. Although the predicted curves agree fairly well with the experimental data, the normalized $(da/dN)_{cf}/(da/dN)_{cf,s}$ data do not appear to fully conform to the predicted linear dependence in $(p_o/2f)$, for

$(p_o/2f) < (p_o/2f)_s$. The probable causes for this discrepancy have been examined thoroughly. The discrepancy is not believed to be attributable to (i) the assumption of an one dimensional model, (ii) the assumption that the reaction time is equal to 1/2f, or (iii) the probable level of water vapor in the reference environment (i.e., in the dehumidified argon used here). The apparent deviation from linearity is believed to result mainly from the large uncertainties involved in the calculation of $(da/dN)_{cf}$. Because $(da/dN)_{cf}$ represents the difference between $(da/dN)_e$ and $(da/dN)_r$, errors tend to be very large, particularly at the lower water vapor pressures. The errors tend to be particularly troublesome for this 2219-T851 aluminum alloy. Because of the relatively mild influence of environment, the $(da/dN)_{cf}$ data can be significantly biased by uncertainties in the measured values of $(da/dN)_r$. In this context, uncertainties in water vapor pressure can also affect the results. To better evaluate the model, materials that are more sensitive to water vapor should be chosen.

In light of these uncertainties, the apparent disagreement is not believed to be significant, and the following observations can be made:

1. The pressures or $p_o/2f$ needed to produce "saturation" are essentially independent of ΔK for each case (i.e., at a given load ratio).

2. The values of $(p_o/2f)_s$ predicted from equation (10), using $\beta^*/\alpha = 3.8$, are in reasonable agreement with the experimental data.
3. The enhancement of crack growth is a linear function of $p_o/2f$ below $(p_o/2f)_s$.

To further evaluate the model, experimental values of $(da/dN)_r$ and $(da/dN)_{cf,s}$ are listed in Tables 1 and 2. Table 1 shows that $(da/dN)_r$ increases with increasing load ratio. This trend is consistent with the fact that the mechanical component, $(da/dN)_r$, is controlled by local deformation at the crack tip, and is expected to increase with mean load at a given ΔK. Table 2 shows that $(da/dN)_{cf,s}$ is independent of R, at the 95 pct confidence level [22]. This is consistent with the fact that the influence of R on the corrosion fatigue component, $(da/dN)_{cf}$, is principally related to its role in modifying gas transport. At saturation, as the surface reaction is limited (i.e., $\theta = 1$), there should be no significant change in $(da/dN)_{cf,s}$ for the cases with different R but same ΔK.

The foregoing discussion suggests that β^*/α is a material constant and can be used to predict $(p_o/2f)_s$ using equation (10). Since $(da/dN)_{cf,s}$ appears to be independent of R, once $(da/dN)_{cf,s}$ is measured at one

load ratio, then $(da/dN)_{cf}$ can be quantitatively predicted for all R. Furthermore, if the values of $(da/dN)_r$ can be defined for all R, then the crack growth rate $(da/dN)_e$ can be predicted for all R.

V. SUMMARY AND CONCLUSIONS

A modification to the model of Weir et al. for surface reaction and transport controlled fatigue crack growth has been developed to account for the effects of load ratio on environmentally assisted crack growth. The modification is based on considerations that load ratio affects gas transport to the crack tip through its influences on the effective crack opening during cyclic loading and the effective length of flow restriction, which is related to the cyclic plastic zone size. Because load ratio affects principally gas transport to the crack tip, only the transport controlled crack growth response would be altered. Experimental verification of modified model has been made by studying the room temperature fatigue crack growth responses at different load ratios for a 2219-T851 aluminum alloy exposed to water vapor.

The principal findings of this investigation are as follows:

1. The pressures or exposures $(p_o/2f)$ needed to produce "saturation", $(p_o/2f)_s$, are essentially independent of ΔK and are lower for the higher load ratios.

2. The "saturation" pressure or exposure as a function of load ratio can be predicted reasonably well from the modified model based on Knudsen flow. An empirical parameter, β^*/α, used in the model to account for surface roughness, localized deformation, appears to be a constant for a given material. For the 2219-T851 aluminum alloy used in this study, β^*/α is approximately equal to 3.8.
3. The rate of fatigue crack growth in an inert environment, $(da/dN)_r$, increases with load ratio at a given ΔK level.
4. The saturation value of the corrosion fatigue component, $(da/dN)_{cf,s}$, is independent of R at a given ΔK level.
5. The enhancement of crack growth, $(da/dN)_{cf}$, is a linear function of $(p_o/2f)$ below $(p_o/2f)_s$.

The modified model, therefore, allows one to compute the corrosion fatigue crack growth response for any load ratio on the basis of measurements made at a single load ratio, provided that the values of $(da/dN)_r$ are known. The results confirm that the effects of load ratio on environment assisted fatigue crack growth can be attributed to two different sources -- one relating to its effect on local deformation at the crack tip and is

reflected through the mechanical component, $(da/dN)_r$, and the other on its role in modifying gas transport and is manifested through the corrosion fatigue component, $(da/dN)_{cf}$.

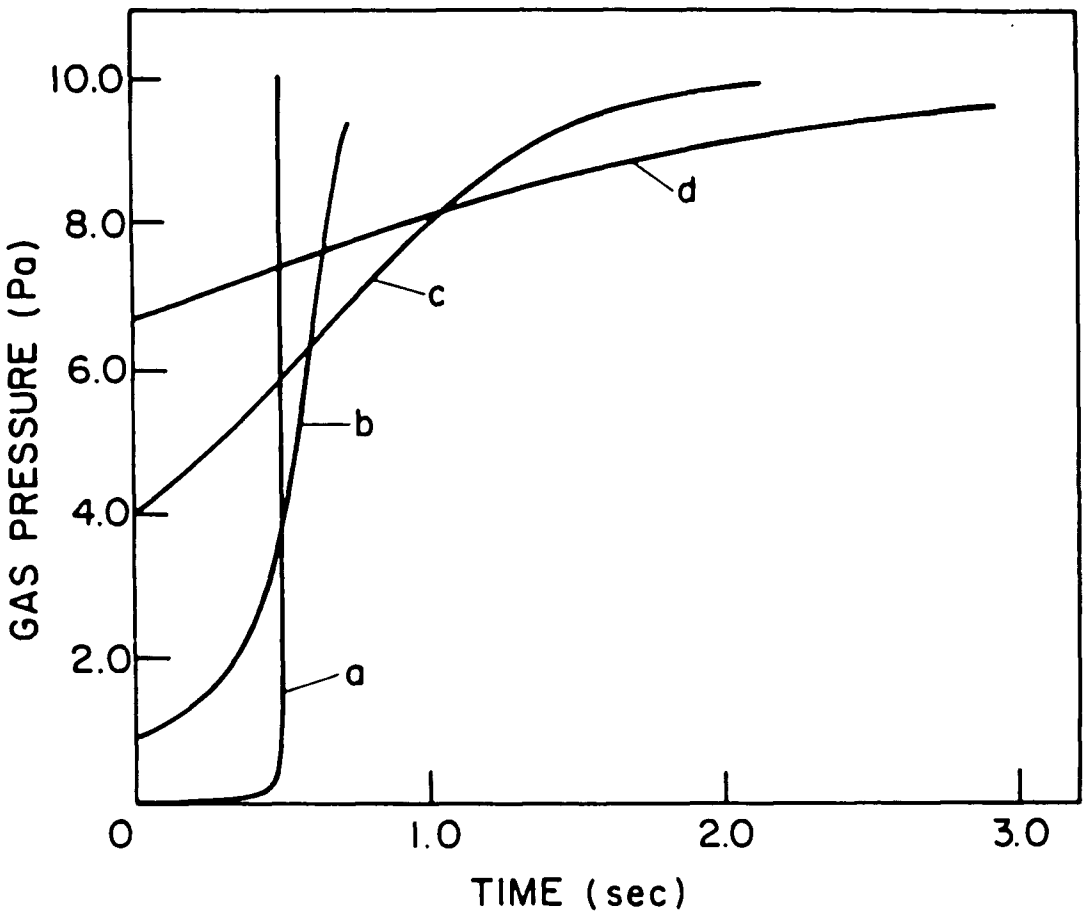

Figure 1: Changes in pressure at the crack tip with time from numerical integration of equations (2) and (3) [7].

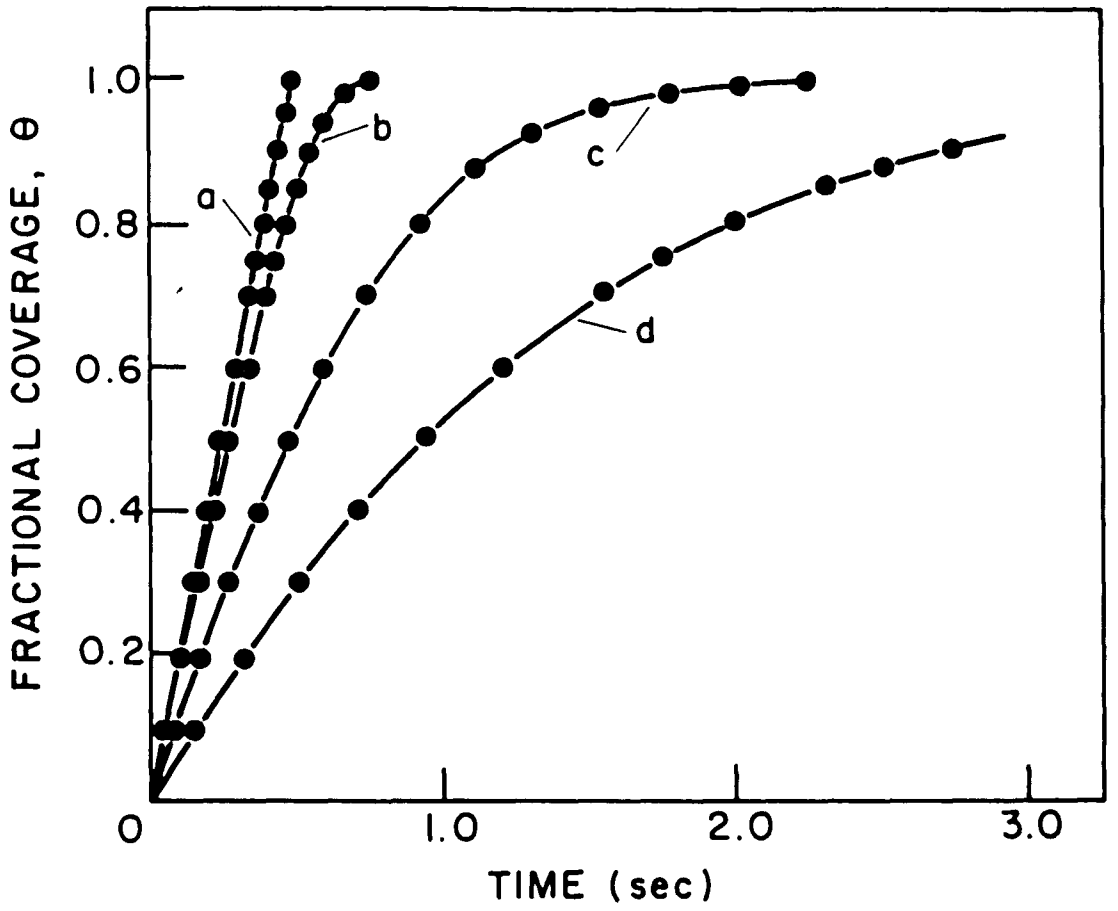

Figure 2: Changes in fractional surface coverage at the crack tip with time from numerical integration of equations (2) and (3) [7].

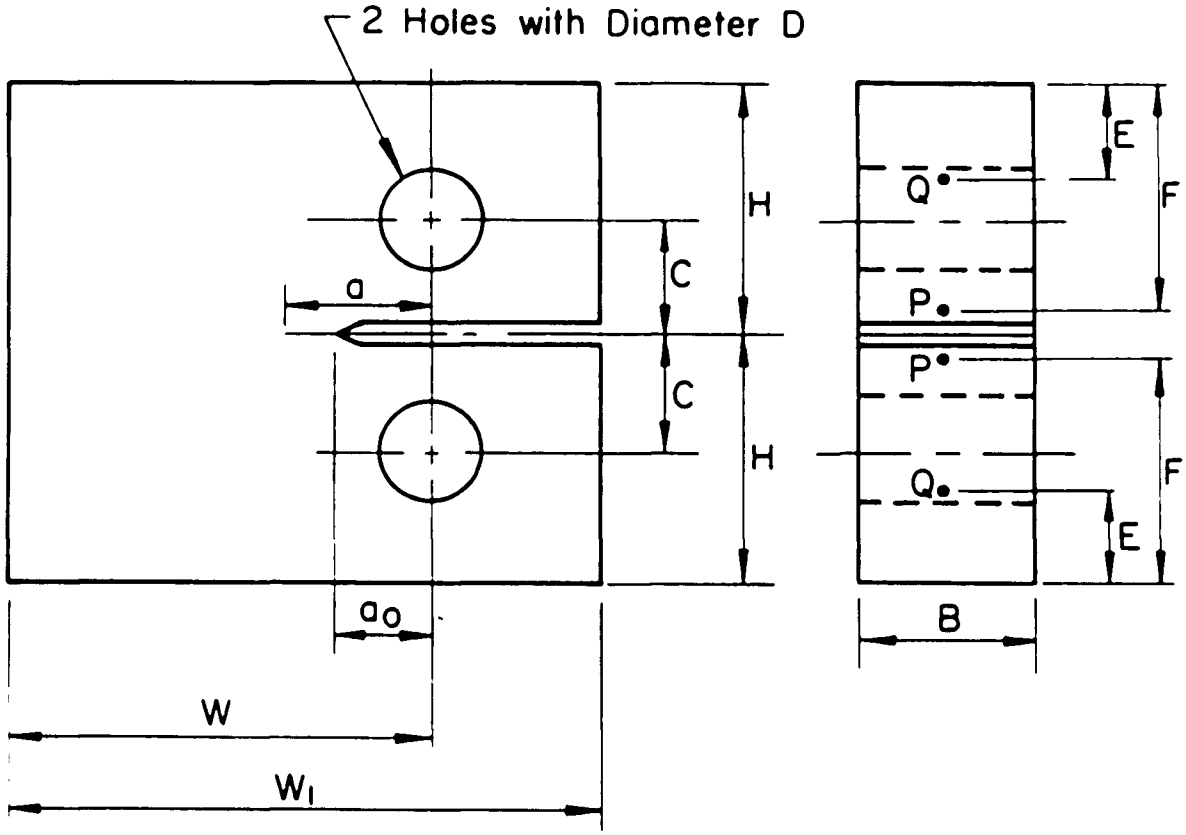

	B	a_o	W	H	W_1	C	D	E	F
mm	16.5	19.6	64.8	31.5	83.8	14.0	15.9	12.4	25.1
in.	0.65	0.77	2.55	1.24	3.30	0.55	0.63	0.49	0.99

P - potential lead connection point

Q - current lead connection point

Figure 3: Wedge opening loading (WOL) specimen for fatigue tests.

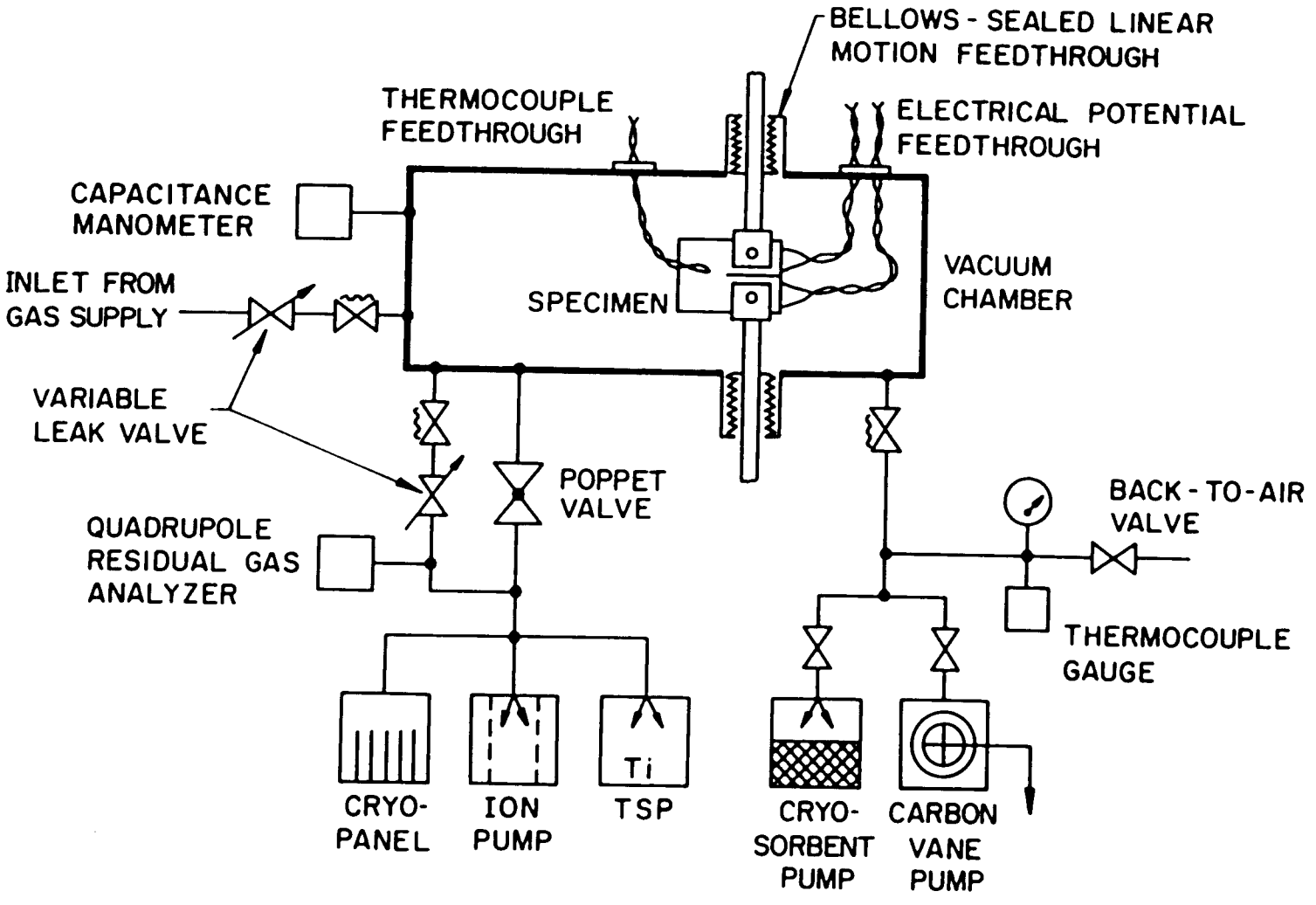

Figure 4: Schematic diagram of the environmental chamber, pumping system and measuring devices [16].

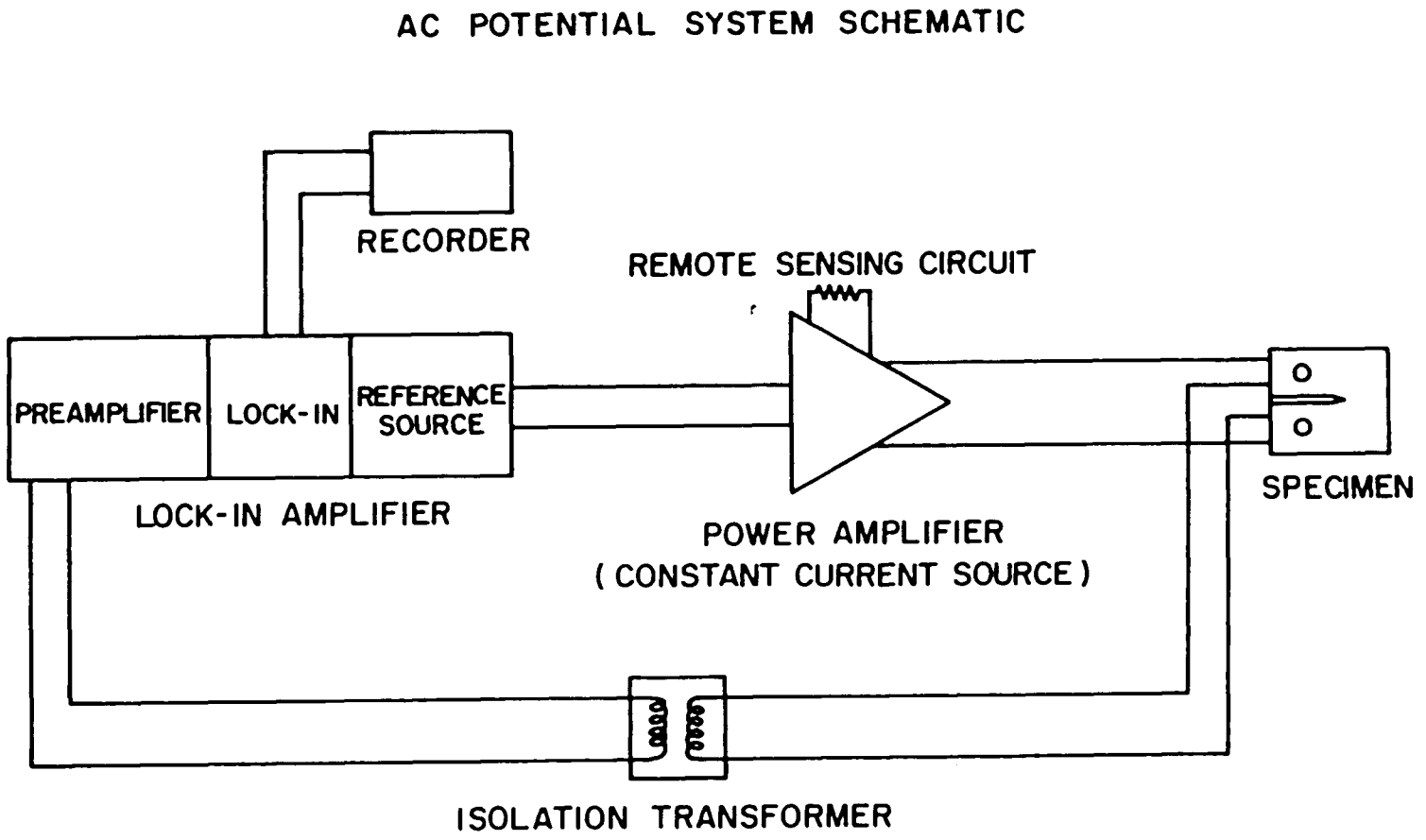

Figure 5: Schematic diagram of the ac potential system for specimen crack length measurements [16].

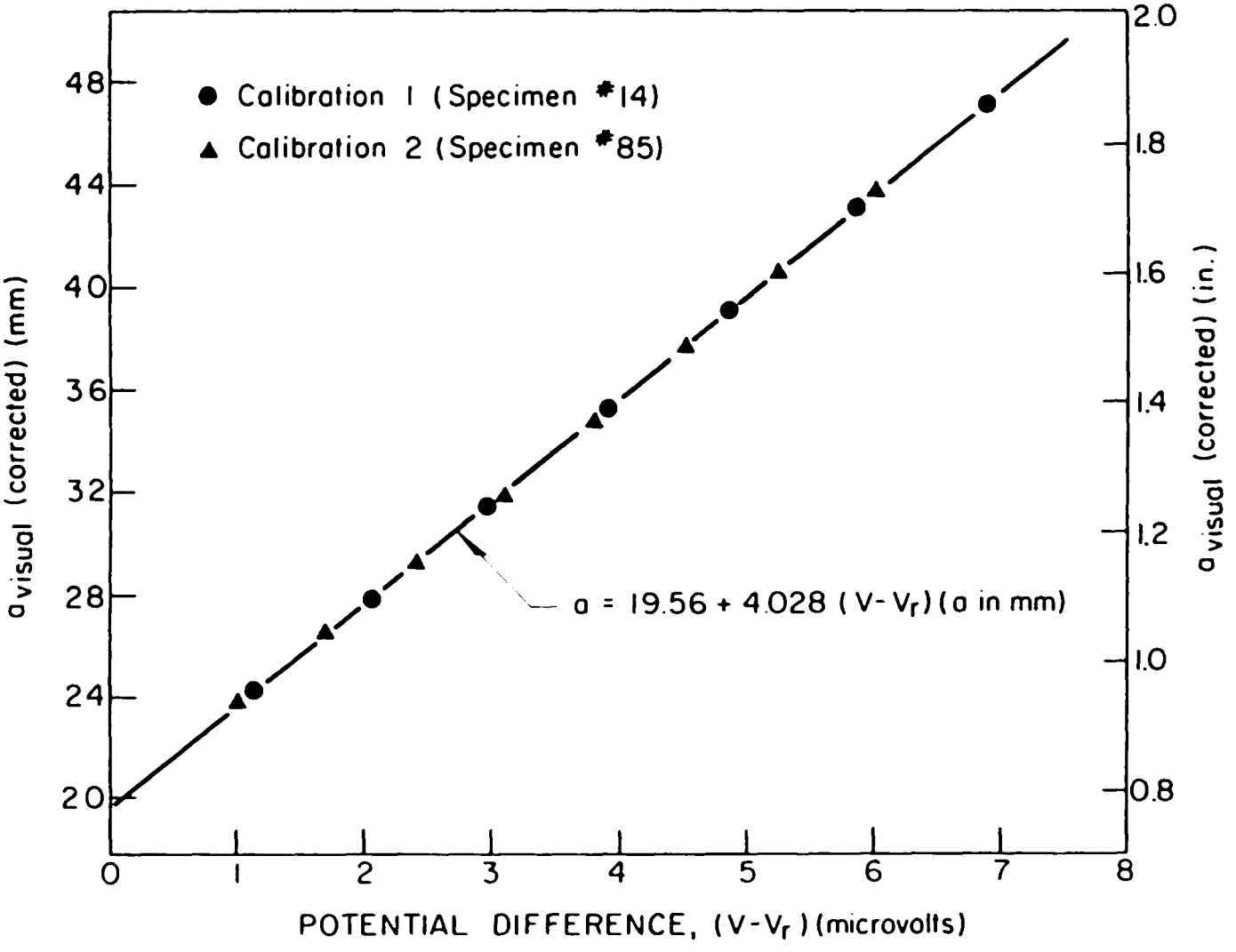

Figure 6: Calibration curve for ac electrical potential crack measurement system [20].

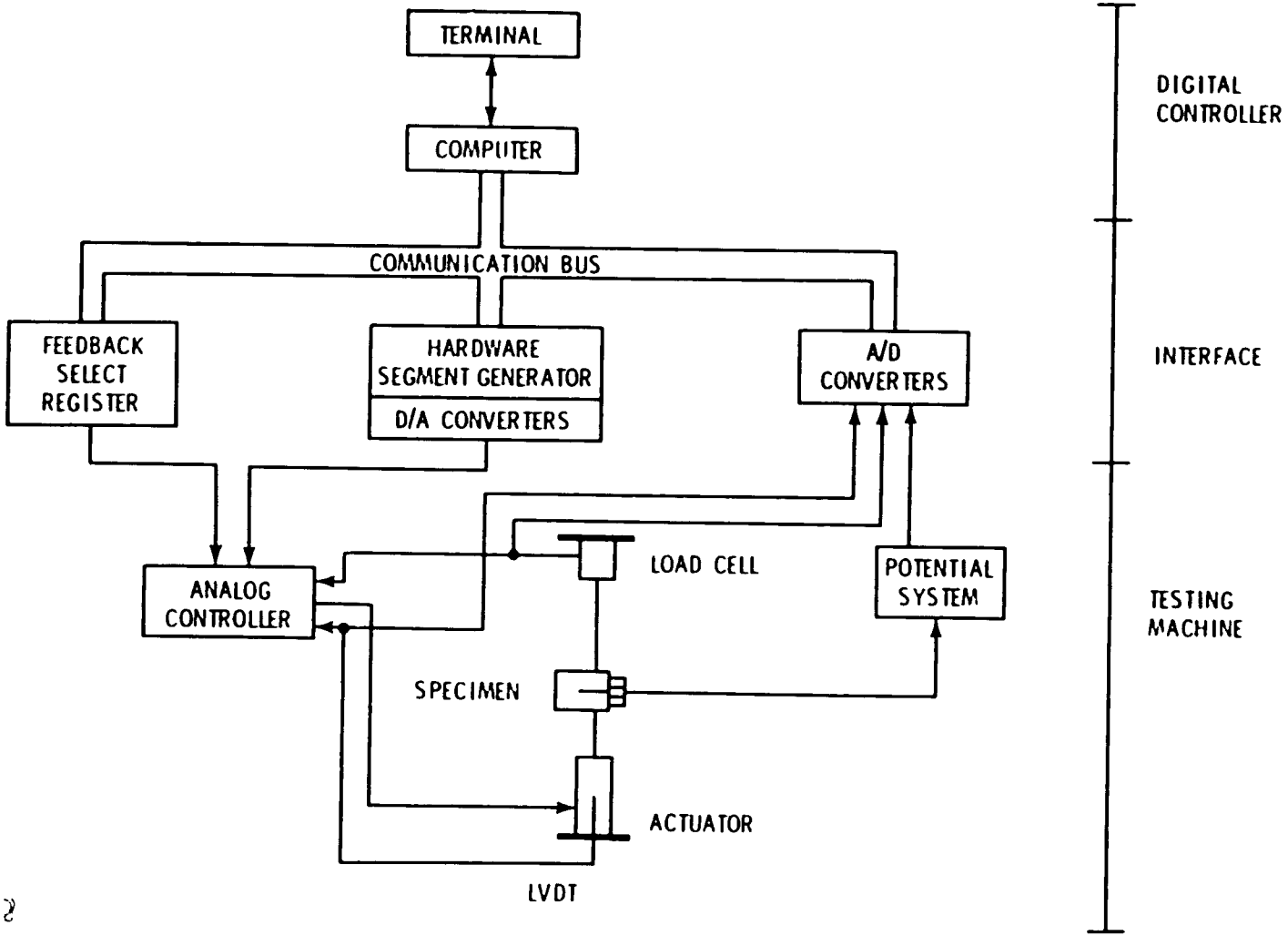

Figure 7: Schematic of the testing machine control electronics connected to the digital controller through the communication interface [16].

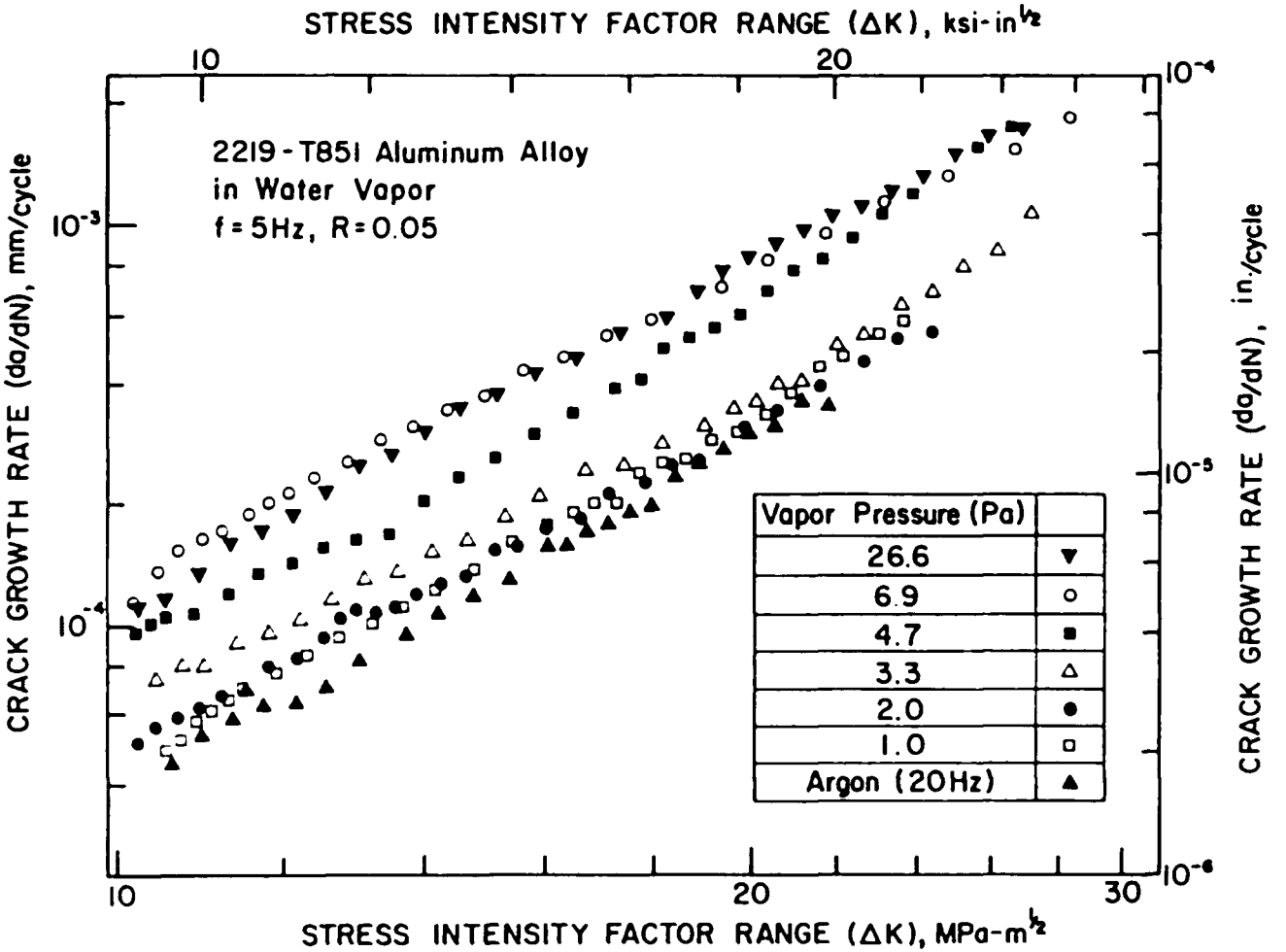

Figure 8: Influence of water vapor pressure on the kinetics of fatigue crack growth with load ratio of 0.05 in 2219-T851 aluminum alloy at room temperature [9].

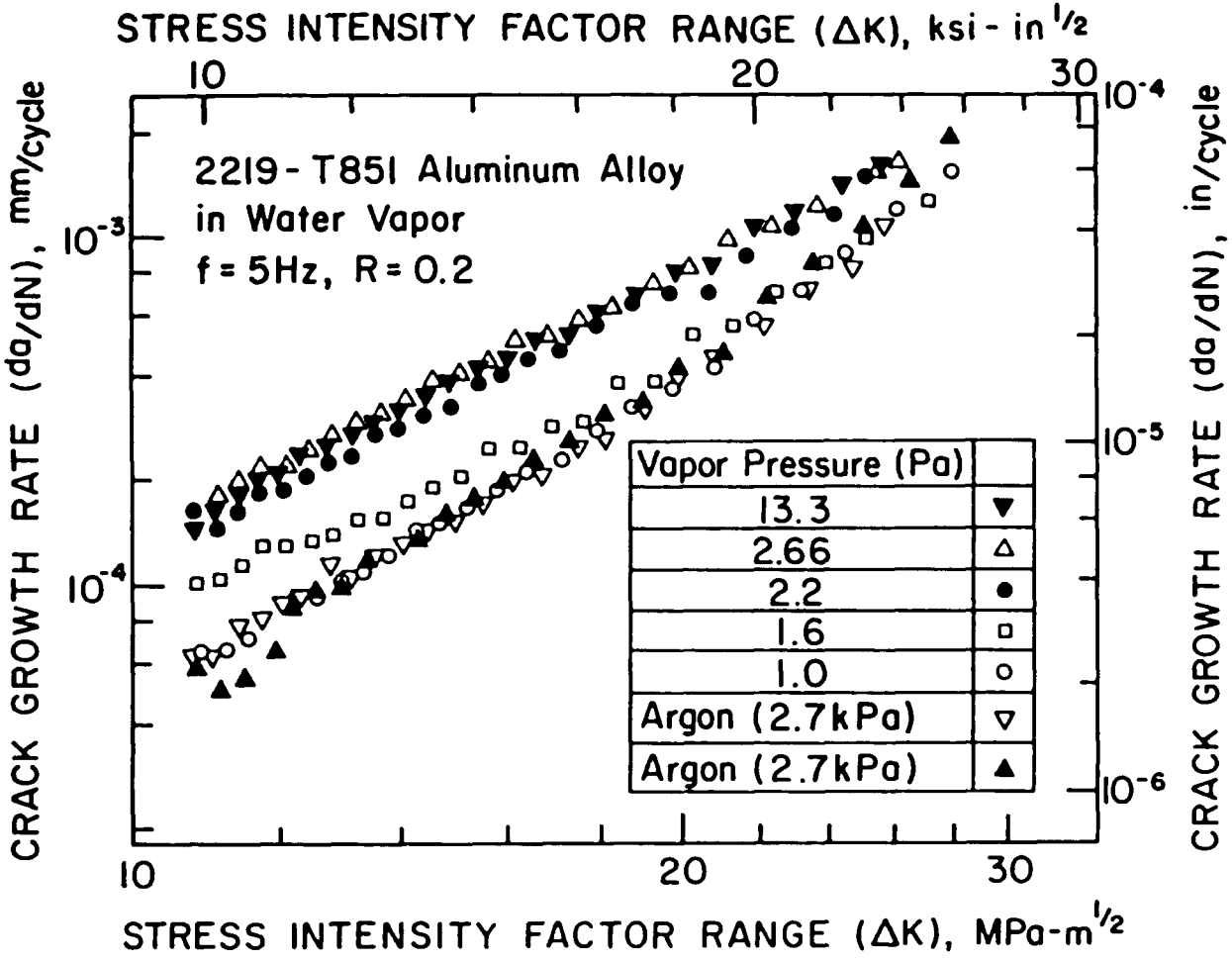

Figure 9: Influence of water vapor pressure on the kinetics of fatigue crack growth with load ratio of 0.2 in 2219-T851 aluminum alloy at room temperature.

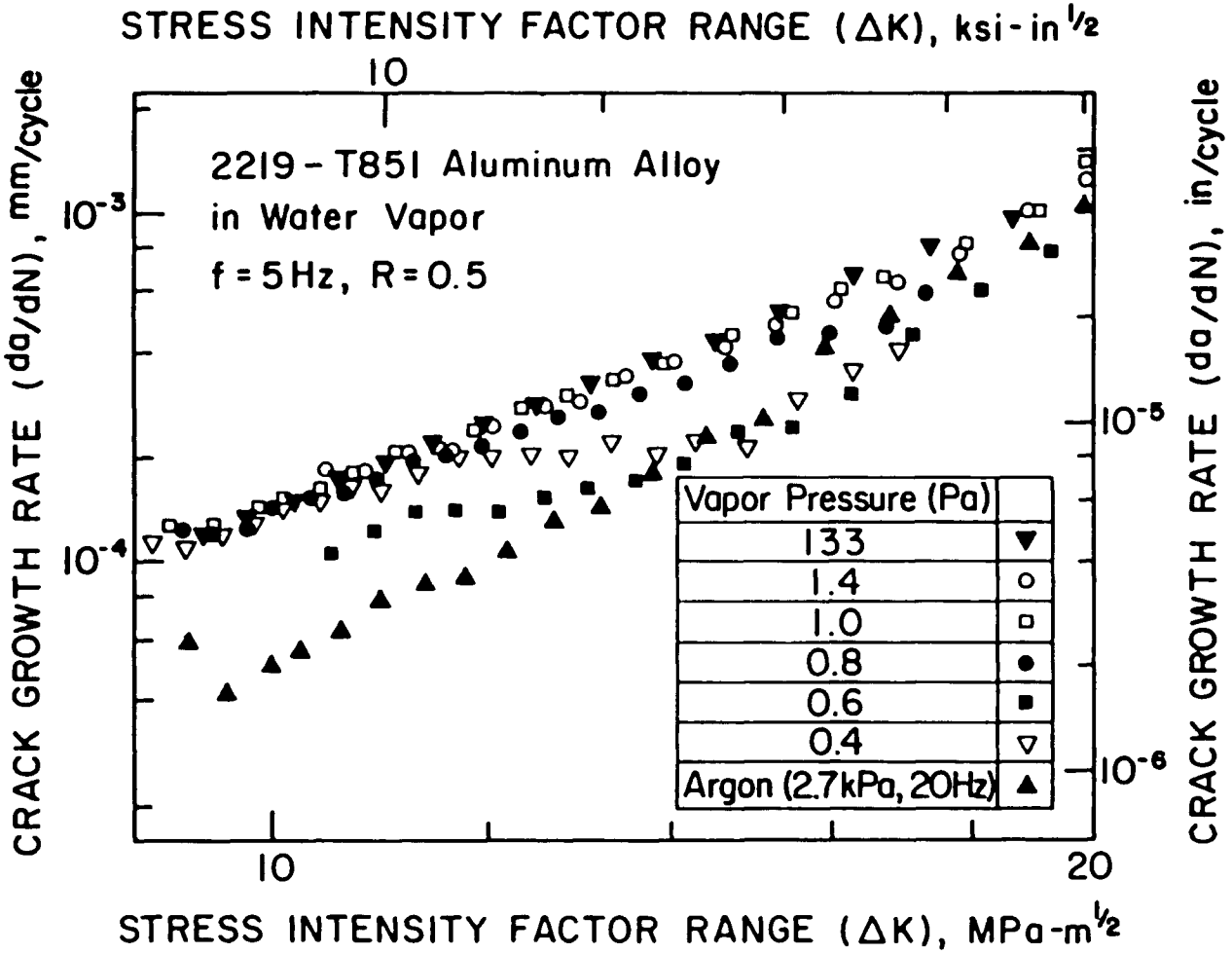

Figure 10: Influence of water vapor pressure on the kinetics of fatigue crack growth with load ratio of 0.5 in 2219-T851 aluminum alloy at room temperature.

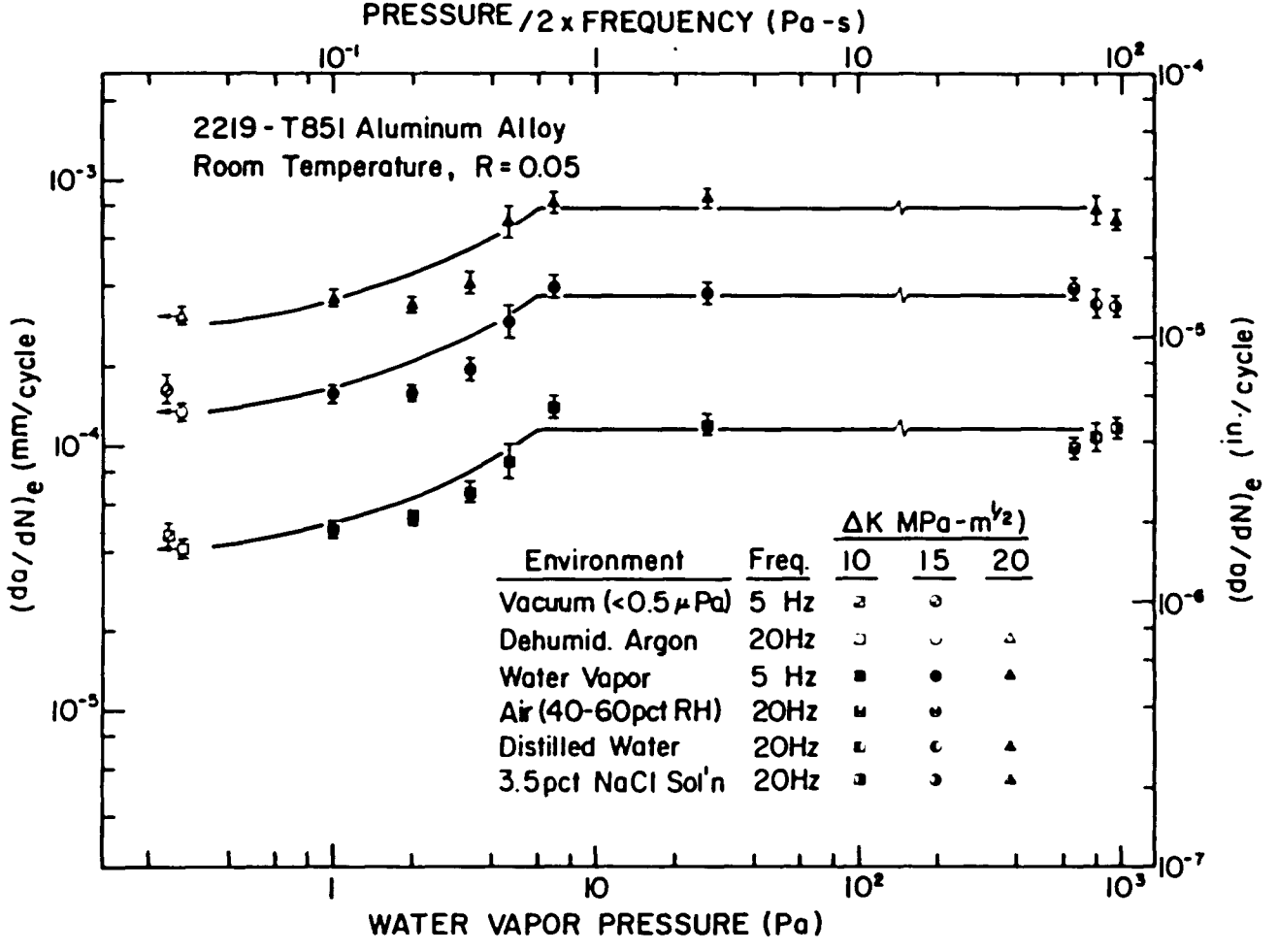

Figure 11: Influence of water vapor pressure (or pressure/2 x frequency) on fatigue crack growth rates with load ratio of 0.05 in 2219-T851 aluminum alloy at room temperature [9].

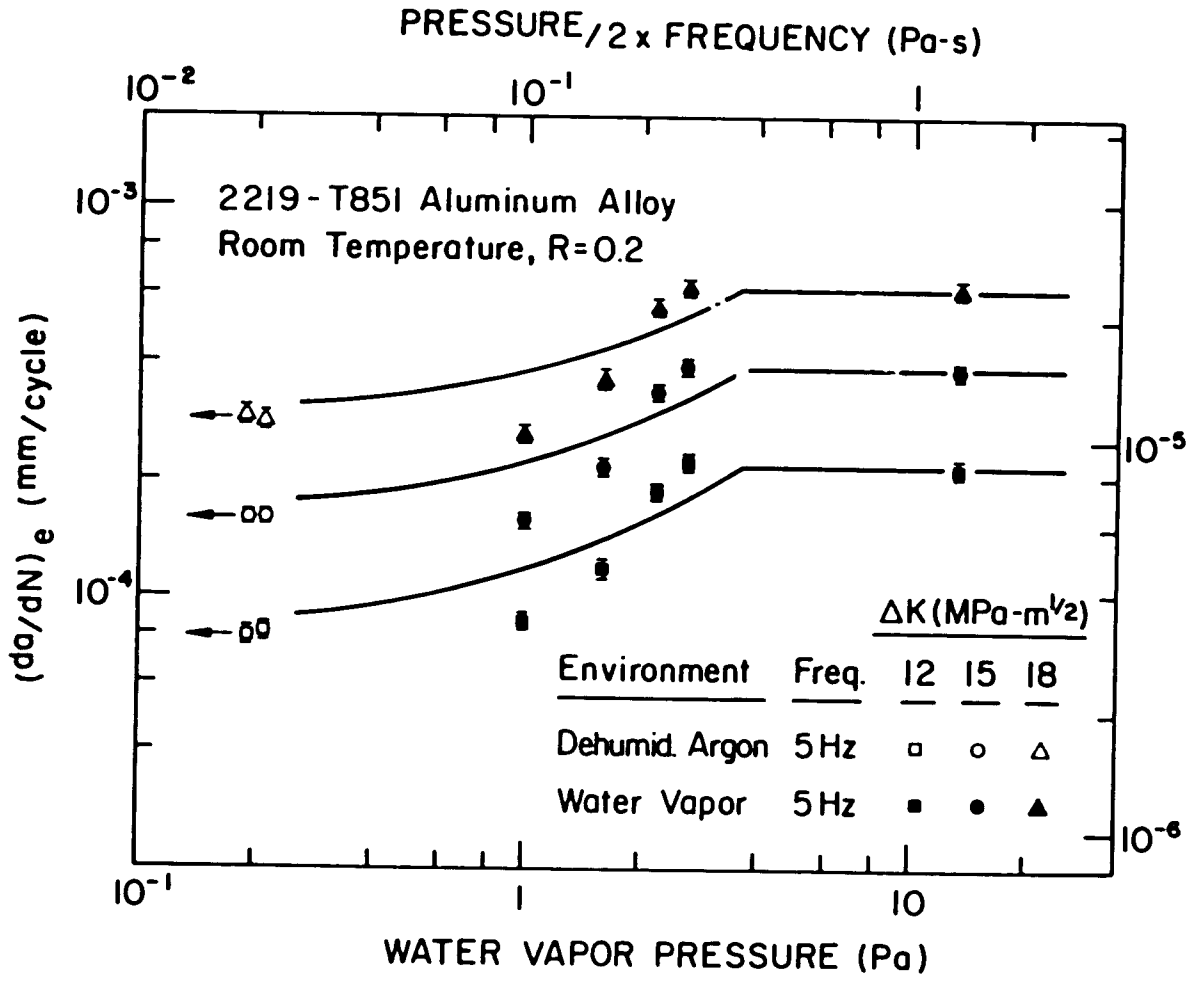

Figure 12: Influence of water vapor pressure (or pressure/2 x frequency) on fatigue crack growth rates with load ratio of 0.2 in 2219-T851 aluminum alloy at room temperature.

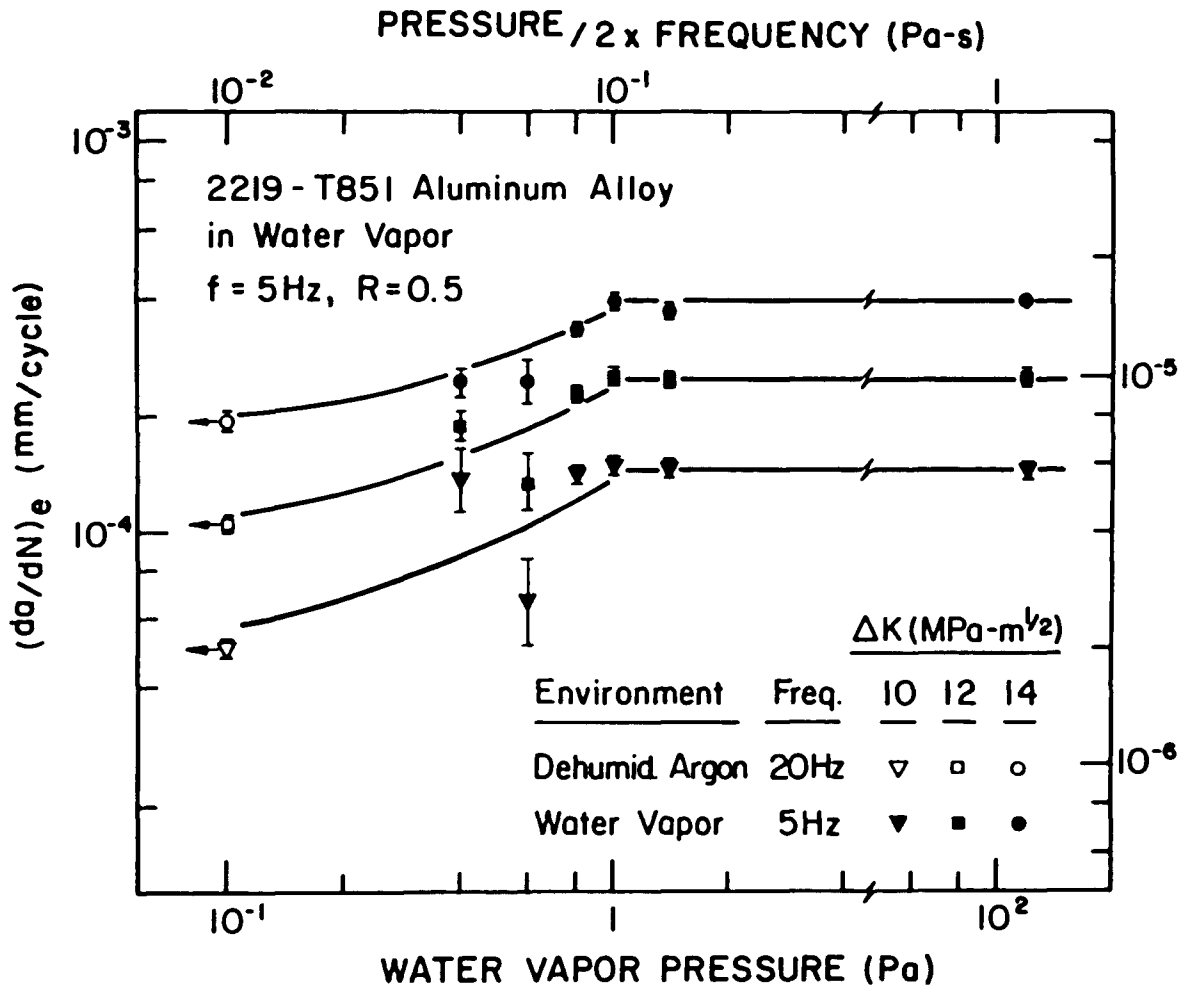

Figure 13: Influence of water vapor pressure (or pressure/2 x frequency) on fatigue crack growth rates with load ratio of 0.5 in 2219-T851 aluminum alloy at room temperature.

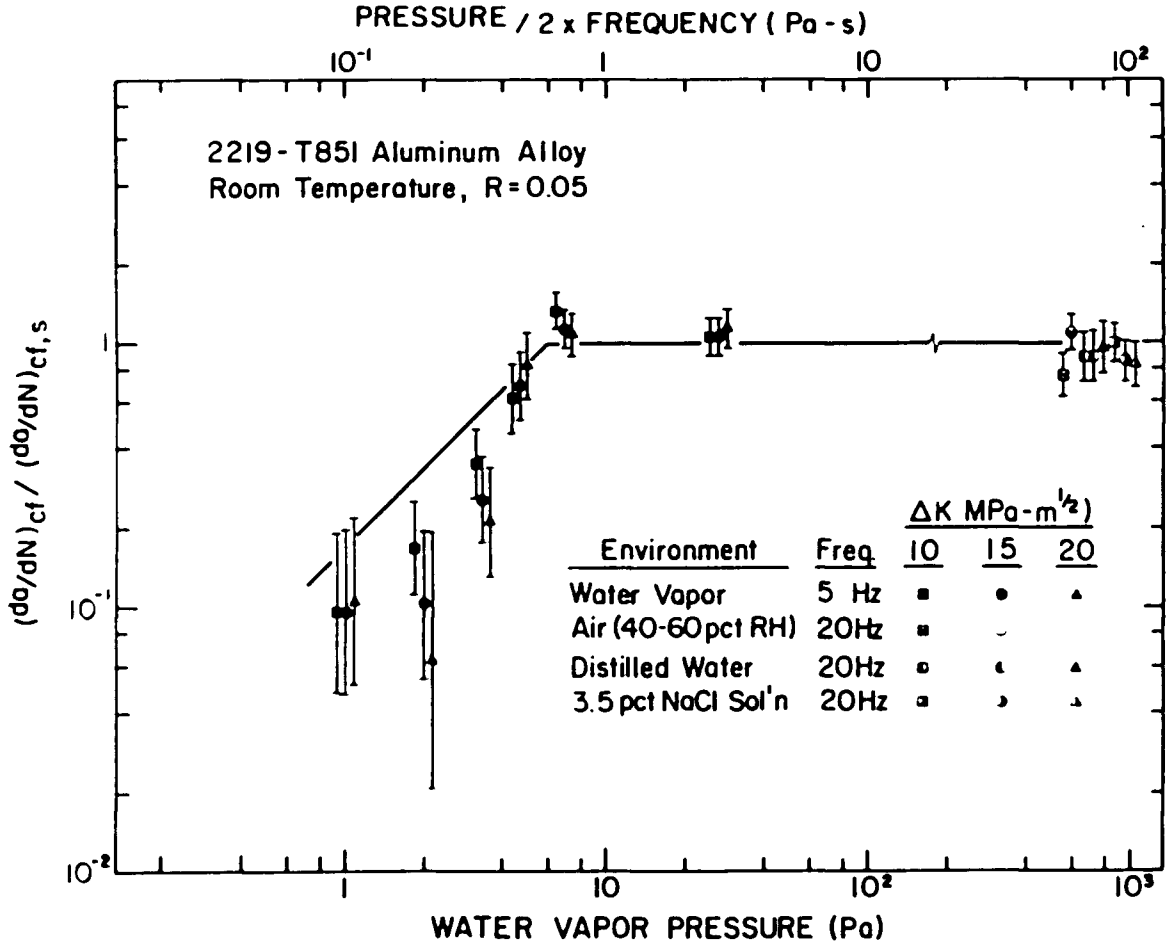

Figure 14: Comparison of normalized corrosion fatigue crack growth rates at load ratio of 0.05 with model predictions for pressure and frequency dependence [9].

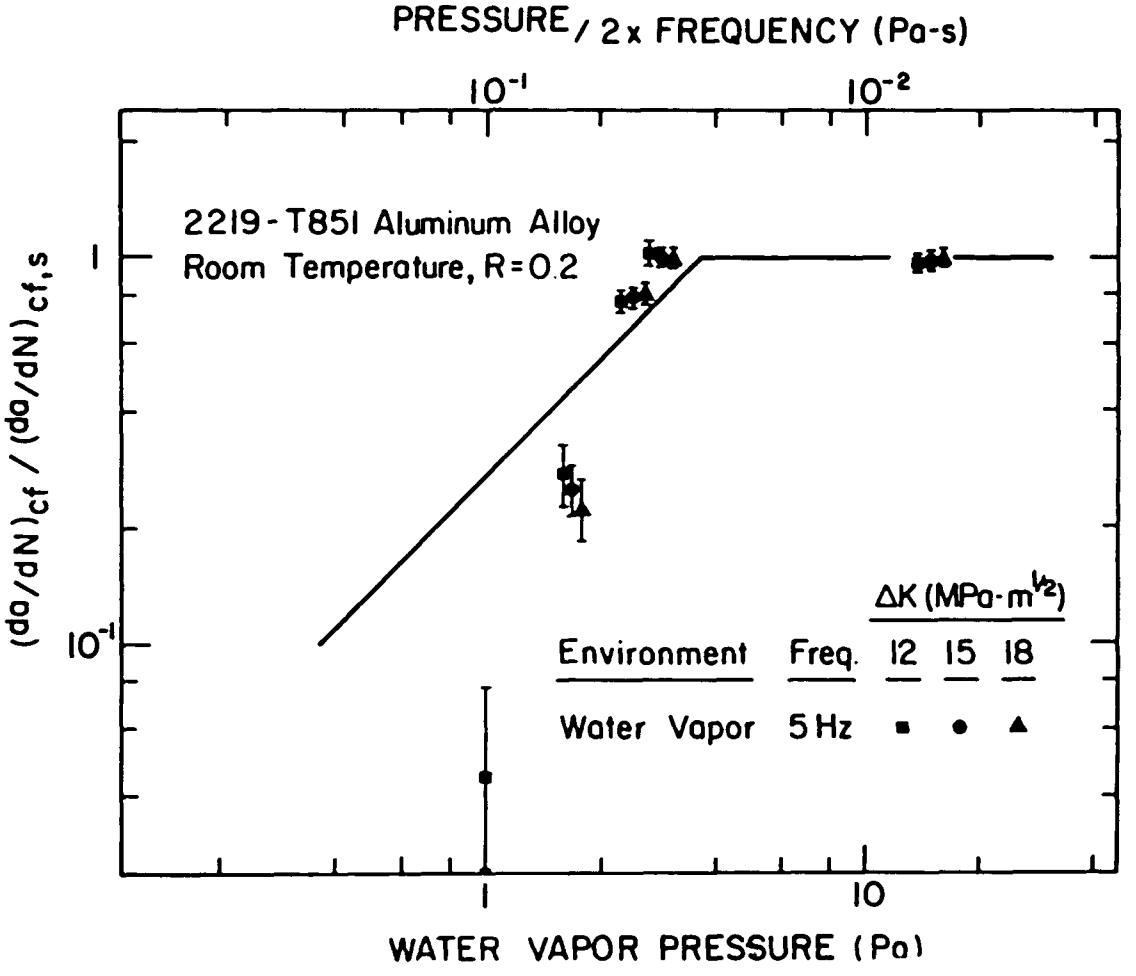

Figure 15: Comparison of normalized corrosion fatigue crack growth rates at load ratio of 0.2 with model predictions for pressure and frequency dependence.

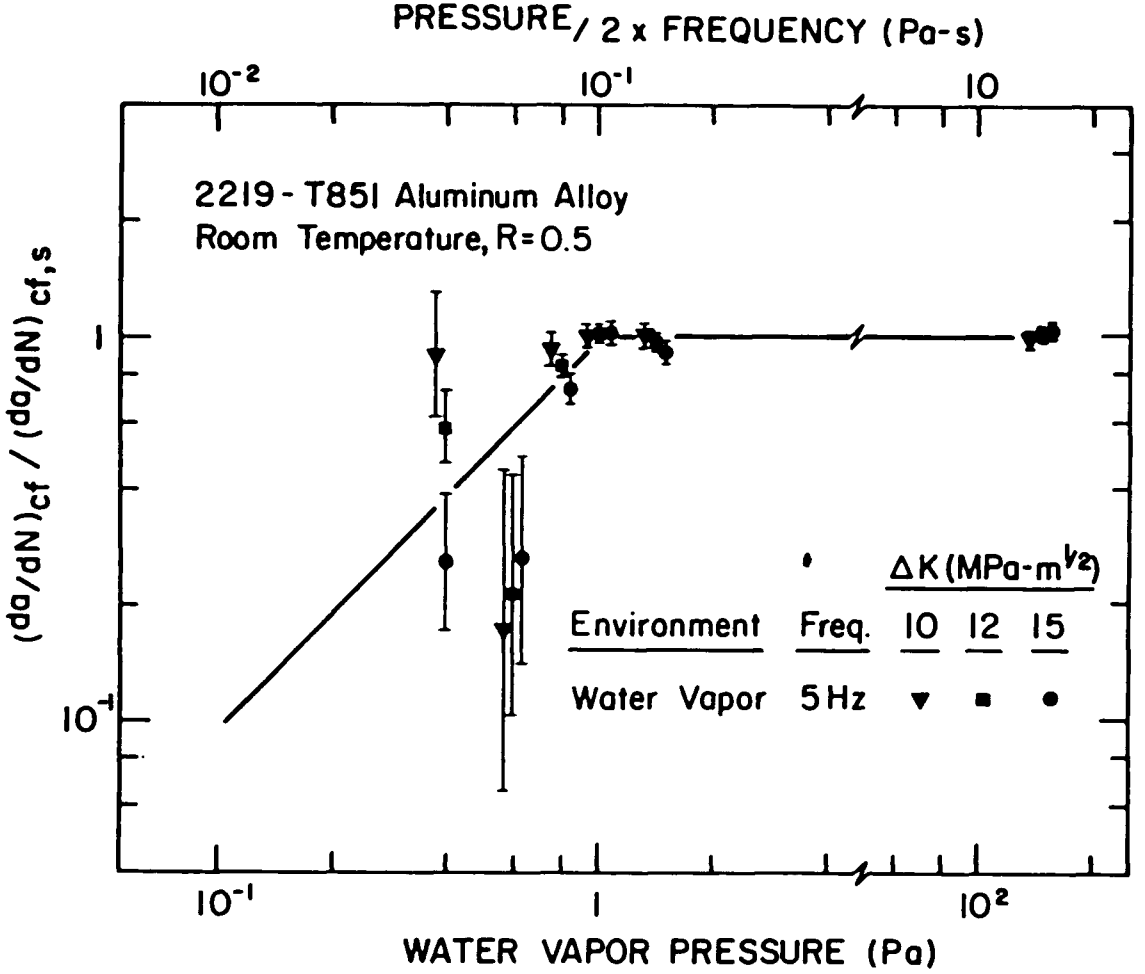

Figure 16: Comparison of normalized corrosion fatigue crack growth rates at load ratio of 0.5 with model predictions for pressure and frequency dependence.

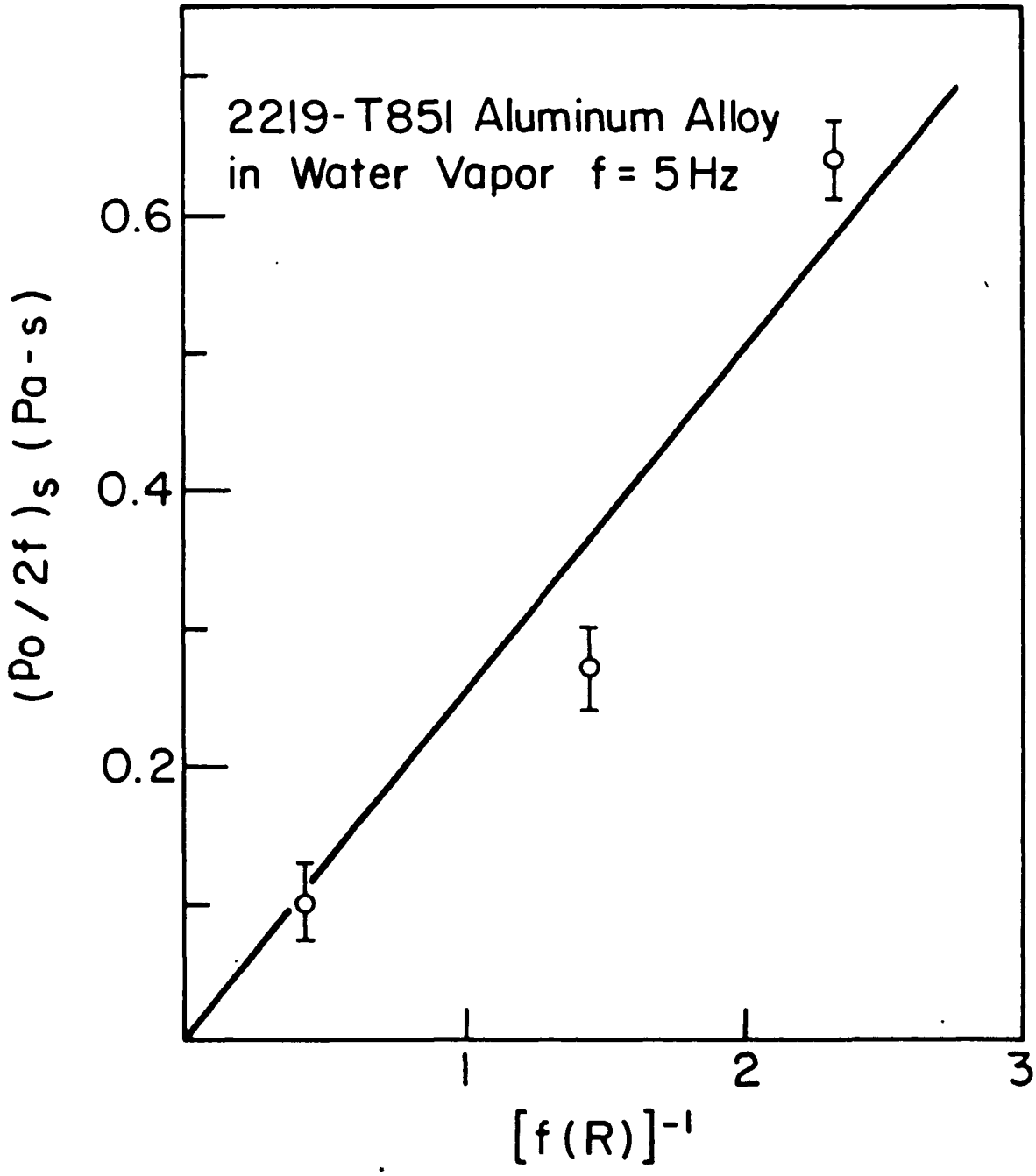

Figure 17: Influence of load ratio on the saturation value of exposure in 2219-T851 aluminum alloy at room temperature. Solid lines represents the best fit to the data.

TABLE I

Fatigue Crack Growth Rate in an Inert Environment (dehumidified argon), $(da/dN)_r$, at different R and ΔK for 2219-T851 aluminum alloy at room temperature.

	$(da/dN)_r$ at indicated ΔK		
R	10	12	15
0.05	3.82	6.40	12.1
0.2	4.41	7.91	16.2
0.2	4.60	8.06	16.0
0.5	5.04	10.4	25.4

TABLE II

Saturation Values of Corrosion Fatigue Component, $(da/dN)_{cf,s}$, at different R, p_o and ΔK for 2219-T851 aluminum alloy at room temperature.

		$(da/dN)_{cf,s}$ at indicated ΔK		
R	p_o	10	12	15
0.05	6.9	8.51	14.2	26.8
0.05	26.6	7.10	11.9	22.4
0.2	2.66	9.47	14.2	22.9
0.2	13.3	8.83	13.4	22.2
0.5	1.0	9.76	14.8	22.9
0.5	1.4	9.62	14.0	20.1
0.5	133	9.44	14.7	23.8

REFERENCES

1. Broek, D. and Schijve, J., "The Influence of the Mean Stress on the Propagation of Fatigue Cracks in Aluminum Alloy Sheets", Nat. Aerospace Inst. Amsterdam TR-M-2111 (1963).

2. Wei, R. P., ASTM 675 "Fatigue Mechanisms", Fong, J. T. ed., Am. Soc. for Testing and Materials (1979), pp. 816-840.

3. Erdogan, F., "Crack Propagation Theories", NASA-CR-901 (1967).

4. Walker, E. K., "Effects of Environments and Complex Load History on Fatigue Life", ASTM STP 462, (1970), pp. 1-14.

5. Walker, E. K., "An Effective Strain Concept for Crack Propagation and Fatigue with Specific Application to Biaxial Stress Fatigue", Air Force Conf. on Fracture and Fatigue (1969). AFFDL-TR-70-144 (1970), pp. 225-233.

6. Forman, R. C., Kearney, V. E. and Engle, R. M., "Numerical Analysis of Crack Propagation in a Cyclic-Loaded Structure" ASME Trans. J. Basic Eng. 89D, (1967) p. 459.

7. Weir, T. W., Simmons, G. W., Hart, R. G., and Wei, R. P., "A Model for Surface Reaction and Transport Controlled Fatigue Crack Growth" scripta Met., 14 (1980), pp. 357-364.

8. Wei, R. P. and Simmons, G. W., "Surface Reactions and Fatigue Crack Growth" Presented at 27th Sagamore Army Materials Research Conference, New York, July, 1980, to be published.

9. Wei, R. P., Simmons, G. W., Hart, R. C., Pao, P. S. and Weir, T. W., "Fracture Mechanics and Surface Chemistry Studies of Fatigue Crack Growth in an Aluminum Alloy" Met. Trans. A, 11A(1980), pp. 151-158.

10. Wei, R. P. and Simmons, G. W., "Recent Progress in Understanding Environment Assisted Fatigue Crack

Growth" Int. J. Fract. 17, pp. 235-247, Apr. 1981.

11. Pao, P. S., Wei, W. and Wei, R. P., "Effect oF Frequency on Fatigue Crack Growth Response of AISI 4340 Steel in Water Vapor", in Environment-Sensitive Fracture of Engineering Materials. TMS-AIME, Z. A. Foroulis, ed., pp. 565-580 (1979).

12. Dushman, S., Scientific Foundations of Vacuum Technique 2nd ed., J. M. Lafferty, ed., p. 88, Wiley (1962).

13. Irwin, G. R., in Structural Mechanics, Pergamon Press, p. 557 (1960).

14. Rice, J. R., "Mechanics of Crack Tip Deformation and Extension by Fatigue" ASTM STP 415, pp. 247-311.

15. Wilson W. K., Westinghouse Research Laboratories, Report No. 60-1B4-BTLFR-R1, 1966.

16. Brazill, Richard L., "The development of a facility for environment-enhanced fatigue crack growth experiments", M. S. thesis, Lehigh University, 1979.

17. Gangloff, R. P. and Wei, R. P., in Fractography in Failure Analysis, ASTM STP 645, ed. Strauss, B. M. and Cullen, W. H., Jr., pp.87-106, 1978.

18. Johnson, H. H., Matls. Res. Std., 6, p. 422, 1966.

19. Li, Che-Yu and Wei, R. P., Matls, Res. Std., 6 p. 392, 1965.

20. Wei, R. P. Fenelli, N. E., Unangst, K. D. and Shih T. T., "Fatigue Crack Growth Response Following a High-Load Excursion in 2219-T851 Aluminum Alloy", J. Engr. Matls. and Tech., Trans. of ASME, 102, pp. 280-292, July 1980.

21. Clark, W. G., Jr. and Hudak, S. J., Jr., J. Testing and Evaluation, 3, no. 6, pp. 454-476, Nov. 1975.

22. Walpole, R. E. and Myers, R. H., Probability and Statistics for Engineers and Scientists 2nd ed., pp. 238-255 Macmillan (1978).

APPENDIX

The r.m.s. Value of Elastic Crack Opening

Based on the considerations that the elastic crack opening varies during cyclic loading and that the flow parameter F depends on δ^2 (see equation (6)), the r.m.s. value of elastic crack opening is used to model the influence of crack opening on flow. For plane strain, the elastic crack opening is given by equation (A-1).

$$\delta_e = \frac{3K\sqrt{\ell}}{E} \qquad \text{(A-1)}$$

Because the change in δ_e is related to the change in stress intensity factor (K) or applied load (P), the r.m.s. value of δ_e is defined in terms of the r.m.s. value of P or K.

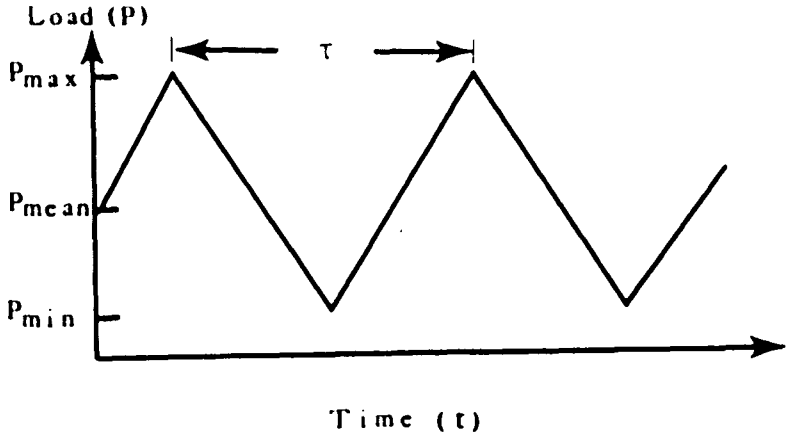

Figure A: Schematic representation of fatigue load components.

For a cyclic loading (see Fig. A) with wave form W(t) and period τ, the variation in load with time, P(t), is expressed by equation (A-2).

$$P(t) = \left[\frac{1 + R}{2} + \frac{1 - R}{2} W(t)\right] P_{max} \qquad (A-2)$$

The r.m.s. value of P is defined by equation (A-3).

$$P_{rms} = \left[\frac{1}{\tau} \int_o^{\tau} P^2(t)\ dt\right]^{1/2} \qquad (A-3)$$

For sinusoidal loading, W(t) is given by $\sin(2\pi t/\tau)$. By substituting P(t) from equation (A-2) into equation (A-3) and integrating the resulting equation, the r.m.s. value of P for sinusoidal loading is obtained.

$$P_{rms} = \frac{1}{2}\left[(1 + R)^2 + \frac{1}{2}(1 - R)^2\right]^{1/2} P_{max} \qquad (A-4)$$

From equations (A-1) and (A-4), the r.m.s. value of δ_e can be expressed as a function of K_{max} and load ratio R.

$$\delta_{rms} = \frac{3 K_{max}\sqrt{\ell}}{E} \frac{1}{2}\left[(1 + R)^2 + \frac{1}{2}(1 - R)^2\right]^{1/2} \qquad (A-5)$$

VITA

The author, TRUE-HWA SHIH, was born in Taiwan, Republic of CHINA on December 27, 1952 to Chung-Chin and Yin-Hsiu Shih. Upon graduation from Chiang-Kuo High School at Taipei, he entered National Central University to pursue a course of study in Civil Engineering in 1972 and received his Bachelor of Science degree in 1976. He served as an Engineering Cfficer in the Chinese Army during 1976-1978.

In January 1979, the author started graduate studies at Lehigh University in the department of Mechanical Engineering and Mechanics. Since then, he has worked under Dr. R. P. Wei studying in the area of environment assisted crack growth of aluminum alloy.

He married the former Ping Lee in May 1980.